

## ORIGINAL ARTICLE

# Loss of phospholipase C $\gamma$ 1 suppresses hepatocellular carcinogenesis through blockade of STAT3-mediated cancer development

Eun-Bi Seo<sup>1,2</sup> | Hyun-Jun Jang<sup>3</sup> | Sun-Ho Kwon<sup>1</sup> | Yong-Jin Kwon<sup>1,2</sup> |  
 Seul-Ki Kim<sup>1</sup> | Song-Hee Lee<sup>1</sup> | Ae Jin Jeong<sup>1</sup> | Hyun Mu Shin<sup>4</sup> |  
 Yong-Nyun Kim<sup>5</sup> | Stephanie Ma<sup>6</sup>  | Haeryoung Kim<sup>7</sup> | Yun-Han Lee<sup>8</sup> |  
 Pann-Ghill Suh<sup>3,9</sup> | Sang-Kyu Ye<sup>1,2,4,10,11</sup>

<sup>1</sup>Department of Pharmacology and Biomedical Sciences, Seoul National University College of Medicine, Seoul, Republic of Korea

<sup>2</sup>Biomedical Science Project (BK21PLUS), Seoul National University College of Medicine, Seoul, Republic of Korea

<sup>3</sup>School of Life Sciences, Ulsan National Institute of Science and Technology, Ulsan, Republic of Korea

<sup>4</sup>Wide River Institute of Immunology, Seoul National University, Hongcheon, Republic of Korea

<sup>5</sup>Division of Translational Science, National Cancer Center, Goyang, Republic of Korea

<sup>6</sup>State Key Laboratory of Liver Research, Li Ka Shing Faculty of Medicine, The University of Hong Kong, Hong Kong

<sup>7</sup>Department of Pathology, Seoul National University College of Medicine, Seoul, Republic of Korea

<sup>8</sup>Department of Molecular Medicine, Keimyung University School of Medicine, Daegu, Republic of Korea

<sup>9</sup>Korea Brain Research Institute (KBRI), Daegu, Republic of Korea

<sup>10</sup>Ischemic/Hypoxic Disease Institute, Seoul National University College of Medicine, Seoul, Republic of Korea

<sup>11</sup>Neuro-Immune Information Storage Network Research Center, Seoul National University College of Medicine, Seoul, Republic of Korea

## Correspondence

Sang-Kyu Ye, Department of Pharmacology, Seoul National University College of Medicine, 103 Daehak-ro, Jongno-gu, Seoul 03080, Republic of Korea.  
 Email: [sangkyu@snu.ac.kr](mailto:sangkyu@snu.ac.kr)

## Funding information

Korea Forest Service, Grant/Award Number: 2020195A00-2122-BA01; National Research Foundation of Korea, Grant/Award Number: NRF-2018R1A5A2025964 and NRF-2022R1A2C1011914; Rural Development Administration, Grant/Award Number: PJ01589402 and PJ01602001; Seoul National University Hospital, Grant/Award Number: 0420200230

## Abstract

Phospholipase C gamma 1 (PLC $\gamma$ 1) plays an oncogenic role in several cancers, alongside its usual physiological roles. Despite studies aimed at identifying the effect of PLC $\gamma$ 1 on tumors, the pathogenic role of PLC $\gamma$ 1 in the tumorigenesis and development of hepatocellular carcinoma (HCC) remains unknown. To investigate the function of PLC $\gamma$ 1 in HCC, we generated hepatocyte-specific PLC $\gamma$ 1 conditional knockout (PLC $\gamma$ 1<sup>ff</sup>; Alb-Cre) mice and induced HCC with diethylnitrosamine (DEN). Here, we identified that hepatocyte-specific PLC $\gamma$ 1 deletion effectively prevented DEN-induced HCC in mice. PLC $\gamma$ 1<sup>ff</sup>; Alb-Cre mice showed reduced tumor burden and tumor progression, as well as a decreased incidence of HCC and less marked proliferative and inflammatory responses. We also showed that oncogenic phenotypes such as repressed apoptosis, and promoted proliferation, cell cycle progression and migration, were induced by PLC $\gamma$ 1. In terms of molecular mechanism, PLC $\gamma$ 1 regulated the activation of signal transducer and activator of transcription 3 (STAT3) signaling. Moreover, PLC $\gamma$ 1 expression is elevated in human HCC and correlates with a poor

This is an open access article under the terms of the [Creative Commons Attribution-NonCommercial-NoDerivs](https://creativecommons.org/licenses/by-nc-nd/4.0/) License, which permits use and distribution in any medium, provided the original work is properly cited, the use is non-commercial and no modifications or adaptations are made.

© 2022 The Authors. *Hepatology Communications* published by Wiley Periodicals LLC on behalf of American Association for the Study of Liver Diseases.

prognosis in patients with HCC. Our results suggest that PLC $\gamma$ 1 promotes the pathogenic progression of HCC, and PLC $\gamma$ 1/STAT3 axis was identified as a potential therapeutic target pathway for HCC.

## INTRODUCTION

Hepatocellular carcinoma (HCC) is a common type of cancer and the fourth leading cause of cancer-related deaths worldwide.<sup>[1]</sup> HCC also accounts for most primary liver cancers. The 5-year survival rate is poor compared with other cancer types, and targeted molecular therapies are difficult to implement due to a lack of biomarkers.<sup>[2]</sup> Over the past decade, chemotherapy for advanced HCC has been limited to sorafenib, and chemoresistance has been common.<sup>[3]</sup> Recently, atezolizumab plus bevacizumab and lenvatinib were approved as first-line therapy for the treatment of unresectable HCC.<sup>[4]</sup> Major risk factors of HCC include infection with hepatitis B virus or hepatitis C virus, excessive alcohol consumption, and nonalcoholic steatohepatitis.<sup>[5]</sup> However, the complex molecular mechanisms underlying the development of HCC remain poorly understood. Therefore, understanding the molecular mechanisms that promote HCC progression is essential for proper diagnosis and treatment.

Phosphoinositide-specific phospholipase C (PLC) is a membrane-associated enzyme that is essential for many cellular processes. PLC is activated by a variety of extracellular ligands to regulate signaling mediated by cellular ligands. PLC hydrolyzes *phosphatidylinositol 4,5-bisphosphate* to generate the second messengers, inositol-1,4,5-triphosphate (IP3) and diacylglycerol (DAG).<sup>[6]</sup> IP3 increases intracellular calcium levels and DAG activates protein kinase C (PKC).<sup>[7]</sup> PLC gamma 1 (PLC $\gamma$ 1), which is 1 of 13 mammalian PLC subtypes, is directly activated by extracellular stimulation to mediate receptor tyrosine kinase signaling.<sup>[8]</sup> Evidence from recent studies suggests that PLC $\gamma$ 1 has an oncogenic function in several cancers. PLC $\gamma$ 1 is highly expressed in several tumors, including breast cancer, colorectal cancer, and gastric cancer.<sup>[9–11]</sup> PLC $\gamma$ 1 also plays a critical role in metastasis and tumor growth.<sup>[12,13]</sup>

Despite efforts to determine the role of PLC $\gamma$ 1 in cancer, little is known about its pathogenic function in HCC, and mechanistic studies are lacking.<sup>[14]</sup> HCC is a major cancer worldwide, so molecular research into its causes is vital. In the present study, we aimed to identify the role and molecular mechanism of PLC $\gamma$ 1 in HCC development. We hypothesized that PLC $\gamma$ 1-deficient mice would be the most useful model to investigate the function of PLC $\gamma$ 1 *in vivo*. However, knockout of PLC $\gamma$ 1 results in embryonic lethality at about embryonic day 9.<sup>[15]</sup> Thus, we generated hepatocyte-specific PLC $\gamma$ 1 conditional knockout mice to determine the

behavior of PLC $\gamma$ 1 in HCC. Then, we induced HCC in both wild-type (WT) and PLC $\gamma$ 1<sup>fl/fl</sup>; Alb-Cre mice using diethylnitrosamine (DEN) and analyzed the pathological phenotypes. Our study has revealed the oncogenic role of PLC $\gamma$ 1 in liver cancer, suggesting a molecular therapeutic target pathway for HCC.

## METHODS

### Mice

Mice were bred and housed in the Animal Research Facility under specific pathogen-free conditions at the Ulsan National Institute of Science and Technology (UNIST). They were maintained under controlled temperature, humidity, and illumination (12-h light/dark cycle) conditions. Standard chow (A03; Scientific Animal Food & Engineering) and water were provided *ad libitum*. The Institutional Animal Care and Utilization Committee approved all of the procedures in accordance with the UNIST guide for the care and use of laboratory animals (UNISTIACUC-14-011).

### Generation of PLC $\gamma$ 1 conditional knockout mice

The *Plcg1*-targeting vector was designed to delete exons 3–5 (“Loxp-exon 3-exon 4-exon 5-Loxp-Frt-Neo-Frt”).<sup>[16]</sup> E14K ES cells were electroporated with the *Plcg1*-targeting vector, and single clones were microinjected into blastocysts. The Frt-Neo cassette was removed by crossing with flippase transgenic mice, and the *Plcg1*-floxed mice were backcrossed to C57BL/6J for at least 10 generations. The *Plcg1*-floxed mice were genotyped using the following primers: forward (5'-GCA CAG ACA GAC TTG GAC-3') and reverse (5'-GTT GCT CAA GGT GAA GGC TCT-3'). To generate the liver-specific *Plcg1* deletion, *Plcg1*-floxed mice were crossed with albumin-Cre transgenic mice (B6.Cg-Tg[Alb-Cre]21Mgn/J; Jackson Laboratory). The controls were sibling littermates.

### Liver tumorigenesis

To achieve chemical-induced hepatocarcinogenesis, mice were intraperitoneally injected with a single dose of DEN (25 mg/kg, N0258-1G; Sigma-Aldrich), and the

controls were injected with saline (0.9% sodium chloride) at postnatal day 15. Male mice were humanely sacrificed at 9 months following injection, and liver tissues and blood were collected.

### Serum analysis and enzyme-linked immunosorbent assay

Mouse blood was collected in heparin-coated round-bottom tubes, and serum was obtained after centrifugation at 3000rpm for 10min. The serum aspartate aminotransferase (AST) and alanine aminotransferase (ALT) concentrations were detected with a mouse AST/ALT activity assay kit (Biovision) according to the manufacturer's instructions. The serum tumor necrosis factor (TNF)- $\alpha$  and interleukin (IL)-6 cytokine levels were measured using mouse TNF- $\alpha$ /IL-6 enzyme-linked immunosorbent assay (ELISA) kits (Abbkine) according to the manufacturer's instructions. Human HCC cell culture supernatants were collected and IL-6 levels were measured using the human IL-6 ELISA development kit (Peprotech) according to the manufacturer's instructions.

### Cell lines and culture

The human HCC cell lines Hep3B and Huh7 were purchased from the ATCC. The cell lines were cultured in Dulbecco's modified Eagle's medium (DMEM) containing 10% heat-inactivated fetal bovine serum (FBS) and 1% penicillin streptomycin solution. The cells were incubated in a humidified atmosphere under 5% CO<sub>2</sub> at 37°C.

### Transfection of small interfering RNAs and plasmids

The small interfering RNAs (siRNAs) against PLC $\gamma$ 1 and negative controls were designed by and purchased from Qiagen. HCC cells were transfected with the siRNAs using Lipofectamine RNAiMAX Transfection Reagent (Invitrogen) according to the forward protocol in the manufacturer's instructions. Cells were harvested 48h after transfection. The pcDNA3.1-PLC $\gamma$ 1 plasmid was provided by UNIST. Plasmids were transfected to the HCC cell lines using Lipofectamine 3000 Transfection Reagent (Invitrogen) according to the manufacturer's instructions. To construct stable cell lines, pcDNA3.1-PLC $\gamma$ 1 was transfected into HCC cells, and cells stably expressing PLC $\gamma$ 1 were selected with G418.

### Colony formation assay

Cells were plated in six-well plates at a density of 500 cells per well. After culturing the cells for 7–14 days,

colonies were fixed with 70% ethanol and stained with 0.1% crystal violet solution.

### Flow cytometry assay

For the cell cycle analysis, cells were washed with phosphate-buffered saline (PBS) and fixed in 75% ethanol at 4°C overnight. Cells were stained with propidium iodide RNase staining solution (BD Biosciences) and analyzed by flow cytometry (BD LSRFortessa; BD Biosciences). For the apoptosis analysis, 5 $\mu$ l annexin V-FITC and 5 $\mu$ l propidium were added to the 100- $\mu$ l cell suspension and incubated for 15min in the dark. The reaction was terminated by the addition of 400 $\mu$ l of binding buffer and analyzed by flow cytometry (BD LSRFortessa).

### Migration and invasion assay

A Transwell assay was performed to assess cell migration and invasion. To analyze migration,  $5 \times 10^4$  cells in serum-free medium were seeded into a Falcon insert with 8- $\mu$ m pore size (Becton-Dickinson) and complete growth medium (DMEM containing 10% FBS and 1% PBS) was added to the lower chamber. For the invasion assay, the inserts were precoated with Matrigel (Corning) before the same assay was performed. After incubation at 37°C for 24–48h, the inserts were fixed and stained using Diff-Quik (Sysmex). Cell migration was also assessed by a wound-healing assay. HCC cells were seeded into a six-well plate at a density of  $1 \times 10^6$  cells per well, and wounds were made using a 200- $\mu$ l pipette tip. At 48h after wound formation, wound recovery was measured.

### Human HCC tissue collection

Twelve pairs of liver tumors and adjacent noncancerous tissue specimens were collected from the Department of Pathology, Seoul National University College of Medicine (Seoul, Korea), with approval from the institutional review board (IRB No. H-2004-152-1118).

### Statistical analysis

Statistical analysis was performed using the GraphPad Prism v.8 software (GraphPad Software, Inc.). Data are presented as means  $\pm$  SD or means  $\pm$  SEM. Fisher's exact test was performed to analyze incidence data. Overall survival (OS) and disease-free survival (DFS) were evaluated by the Kaplan–Meier and log-rank tests. The Mann–Whitney U test or two-tailed unpaired Student's *t* test was performed to compare the

differences between two groups.  $p$  values  $<0.05$  were taken as statistically significant.

## RESULTS

### Generation of hepatocyte-specific PLC $\gamma$ 1 knockout mice and induction of HCC by DEN

To examine the potential role of PLC $\gamma$ 1 in HCC, we generated a hepatocyte-specific PLC $\gamma$ 1 conditional deficient mouse model using PLC $\gamma$ 1 floxed mice and Albumin-Cre mice (Figure S1A; see Materials and Methods). Immunoblotting analysis confirmed that PLC $\gamma$ 1 expression was depleted in the liver, but not in other organs (Figure S1B). In addition, messenger RNA (mRNA) expression levels of liver extract were effectively decreased in PLC $\gamma$ 1<sup>ff</sup>; Alb-Cre mice compared with WT mice (Figure S1C). To chemically induce hepatocarcinogenesis, mice were injected with a single dose of DEN at postnatal day 15. The mice were sacrificed, and liver tissues were collected 9 months after injection (Figure 1A; see Materials and Methods). PLC $\gamma$ 1 protein expression of the liver extract was completely abolished in only the PLC $\gamma$ 1<sup>ff</sup>; Alb-Cre mice, in both the saline-treated and DEN-treated groups (Figure S1D). To verify PLC $\gamma$ 1 depletion in the hepatocytes, immunostaining of the liver tissues was performed; the immunohistochemistry intensity results confirmed the absence of PLC $\gamma$ 1 in the PLC $\gamma$ 1<sup>ff</sup>; Alb-Cre mice groups (Figure S1E). In particular, the immunofluorescence results showed that PLC $\gamma$ 1 (green, anti-PLC $\gamma$ 1) was not expressed in hepatocytes (red, anti-Albumin) in the PLC $\gamma$ 1<sup>ff</sup>; Alb-Cre mice groups (Figure 1B). PLC $\gamma$ 1 was also removed from female mice (Figure S2A–C). As a first step, we generated mice in which PLC $\gamma$ 1 was effectively removed from the hepatocytes.

### Loss of PLC $\gamma$ 1 suppresses tumorigenesis and the development of DEN-induced primary liver cancer in mice

To determine the oncogenic role of PLC $\gamma$ 1 in liver malignancy, we assessed the effect of PLC $\gamma$ 1 deletion on HCC *in vivo*. Remarkably, hepatocyte-specific deletion of PLC $\gamma$ 1 decreased tumorigenesis and the tumor burden in the liver (Figure 1C). All WT male mice developed visible hepatic tumors, but only two of the seven PLC $\gamma$ 1<sup>ff</sup>; Alb-Cre mice presented with small and few tumor nodules (Figure 1D). In the saline group, tumors did not develop in any WT or PLC $\gamma$ 1<sup>ff</sup>; Alb-Cre mice. Similarly, female mice did not develop DEN-induced HCC (Figure S2D,E). Analysis of the liver showed that PLC $\gamma$ 1 deletion noticeably reduced the number, volume,

and size of DEN-induced liver tumors (Figure 1E–G). Next, we performed immunohistochemistry to detect proliferating cell nuclear antigen (PCNA) in the liver tissues and assess the proliferation response. Compared with liver tissues from the control mice, the tumors derived from the DEN-treated WT mice had considerably increased PCNA-positive hepatocytes. Remarkably, there were few PCNA-positive cells in the tumors derived from the DEN-treated PLC $\gamma$ 1<sup>ff</sup>; Alb-Cre mice (Figure 1H; Figure S3A). These results indicated that PLC $\gamma$ 1 deletion significantly reduced the number of proliferating tumor cells, suggesting that PLC $\gamma$ 1 mediates hepatic carcinoma growth. Furthermore, we performed Masson's trichrome (MT) staining to evaluate the formation of tumor fibrosis by detecting collagen fibers in liver tissues. MT staining revealed that the formation and progression of fibrotic areas only occurred in the DEN-treated WT mice, and not in the control mice or DEN-treated PLC $\gamma$ 1<sup>ff</sup>; Alb-Cre mice (Figure 1I; Figure S3B). Collectively, these results demonstrated that loss of PLC $\gamma$ 1 in hepatocytes significantly suppressed tumor formation and growth, and that PLC $\gamma$ 1 can be considered to play a critical role in tumorigenesis and the development of HCC.

### PLC $\gamma$ 1 deficiency attenuates the DEN-induced inflammatory response and liver injury in mice

Histological examination using hematoxylin and eosin staining confirmed tumor formation in the liver tissues of the DEN-treated mice. In particular, the tumors from DEN-treated WT mice showed marked inflammatory responses. In these tumors, the trabecular architecture was lost, and we observed inflammatory cell infiltration and eosin-positive cytoplasmic inclusions. These features were not observed in the control or DEN-treated PLC $\gamma$ 1<sup>ff</sup>; Alb-Cre mice (Figure 2A). Tumors were not generated in female mice in any of the groups, but abnormal hepatocytes were observed in WT mice treated with DEN. Dysplastic foci include hepatocytes with atypical morphology such as multinucleated, massive nucleated, and giant cells. These preneoplastic foci did not appear in PLC $\gamma$ 1<sup>ff</sup>; Alb-Cre mice even after DEN treatment (Figure S4A). To confirm liver inflammation and injury, we measured serum concentrations of ALT and AST (hepatic enzymes) by enzyme activity analysis. Serum ALT and AST levels were significantly increased following DEN treatment but recovered to control levels following the deletion of PLC $\gamma$ 1 (Figure 2B,C). We also investigated TNF- $\alpha$  and IL-6 (hepatic inflammatory cytokines), both of which were increased in the DEN-treated WT mice, but which were reduced by knockout of PLC $\gamma$ 1 (Figure 2D,E). These results were confirmed by quantitative reverse-transcription polymerase chain reaction analysis of TNF- $\alpha$  and IL-6 transcripts in mouse

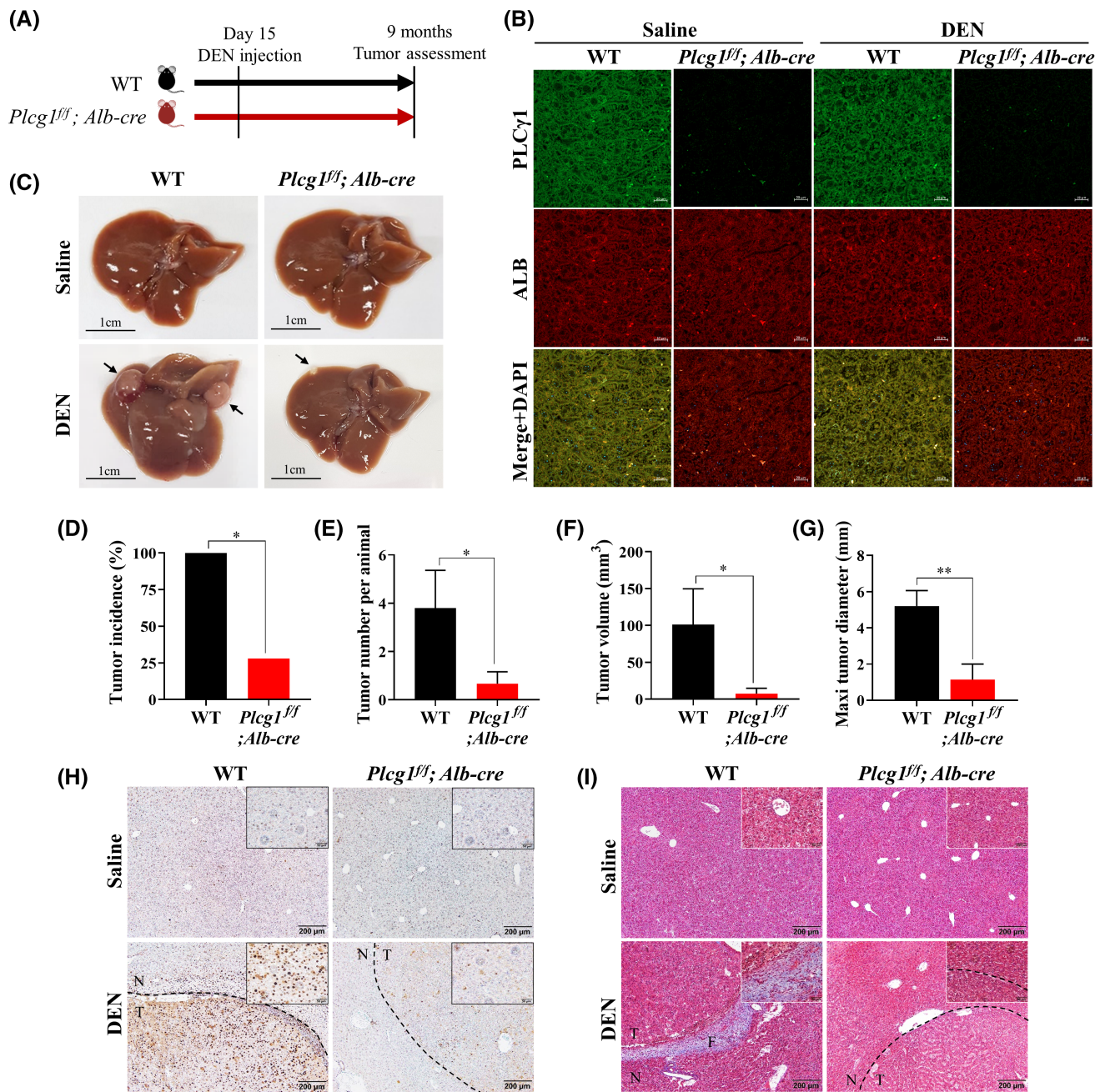


**FIGURE 1** Loss of phospholipase C gamma 1 (PLC $\gamma$ 1) suppresses the tumorigenesis and development of diethylnitrosamine (DEN)-induced primary liver cancer in mice. (A) Scheme of experimental design for DEN-induced mice model of hepatocellular carcinoma (HCC). Wild-type (WT) or PLC $\gamma$ 1<sup>fl/fl</sup>; Alb-Cre mice were injected with DEN (25 mg/kg) or saline (0.9% NaCl) at 2 weeks of age. At 9 months following injection, mice were sacrificed and liver was analyzed. (B) Immunofluorescence staining for PLC $\gamma$ 1 (green), albumin (red), and 4',6-diamidino-2-phenylindole (DAPI; blue) were performed in liver from four groups of mice. (C) Representative images of liver from mice and arrows indicate the tumor nodules. (D) Tumor incidence (statistic was performed using Fisher's exact test). (E) Tumor number per animal. (F) Average tumor volume. (G) Average maximum tumor diameter was compared in DEN-treated WT and PLC $\gamma$ 1<sup>fl/fl</sup>; Alb-Cre mice. Values are expressed as mean  $\pm$  SEM. Statistics were performed using Student's *t* test. (E–G) \**p* < 0.05, \*\**p* < 0.01. (H) Representative images of immunohistochemistry for proliferating cell nuclear antigen (PCNA) in liver tissues. Dashed lines present the border between tumor region and adjacent nontumor. (I) Representative images of Masson trichrome staining in liver tissues. Blue color indicates collagen fiber. F, fibrous area; N, nontumor; T, tumor.

livers (Figure 2F,G). Interestingly, the same trend was observed in female mice, with lower absolute values (Figure S4B,C). We also confirmed the activation of nuclear factor-kappa B (NF- $\kappa$ B) and signal transducer and activator of transcription 3 (STAT3), transcription factors

mediating inflammatory responses. Immunostaining demonstrated that both activated NF- $\kappa$ B (serine 536 phosphorylation) and STAT3 (tyrosine 705 phosphorylation) was prominently expressed in the hepatocytes' nuclei of DEN-treated WT mice and not in PLC $\gamma$ 1<sup>fl/fl</sup>;

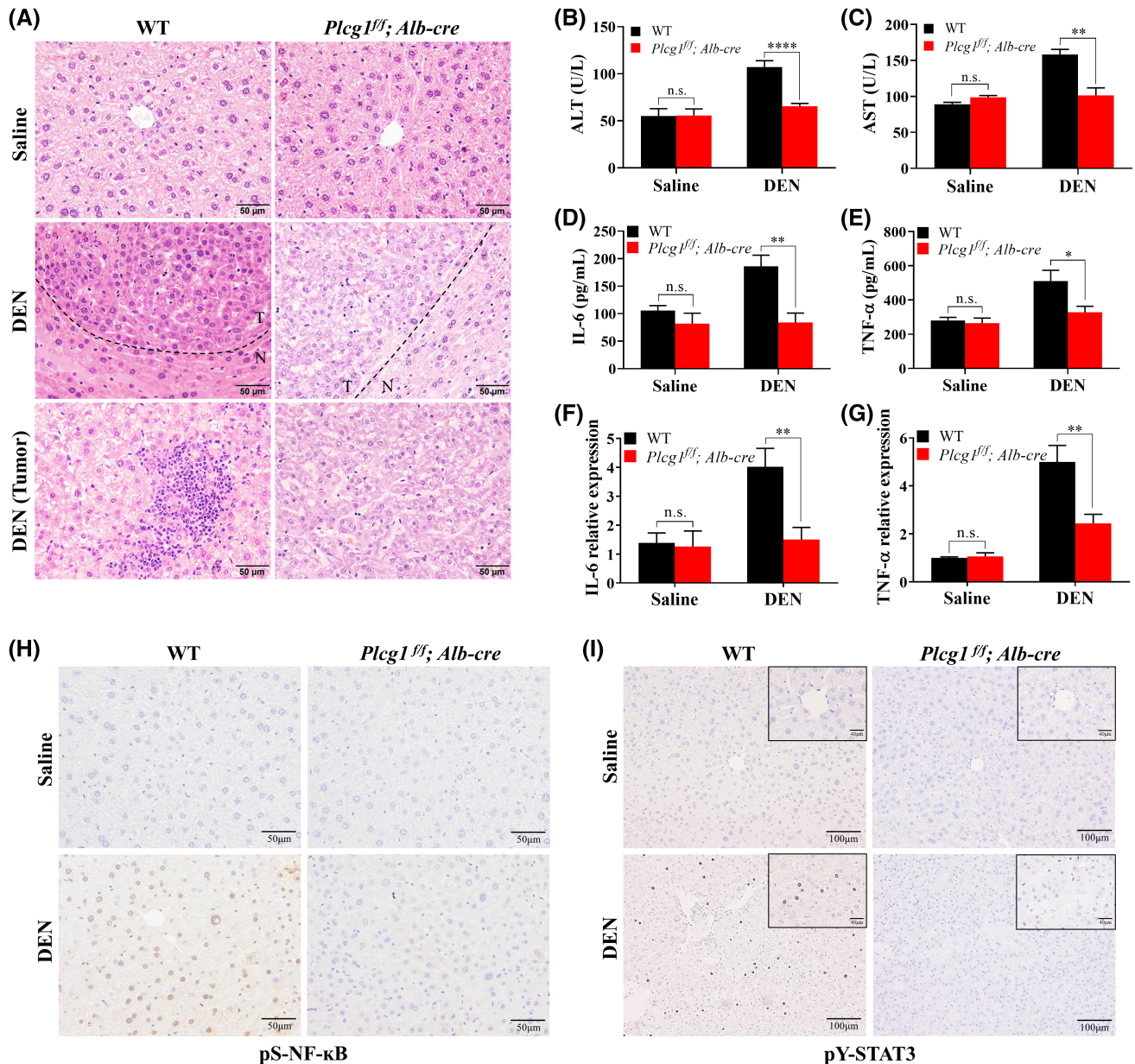


**FIGURE 2** PLC $\gamma$ 1 deficiency attenuates DEN-induced inflammatory response and liver injury in mice. (A) Representative hematoxylin and eosin-stained images of liver tissues from mice. Tumor nodules are outlined and labeled. Tumors from WT liver showed infiltrate of inflammatory cells and eosin-positive cytoplasmic inclusions. Serum alanine aminotransferase (ALT) (B) and aspartate aminotransferase (AST) (C) levels were measured in the four groups of mice. Serum interleukin-6 (IL-6) (D) and tumor necrosis factor- $\alpha$  (TNF- $\alpha$ ) (E) levels were measured by enzyme-linked immunosorbent assay (ELISA). IL-6 (F) and TNF- $\alpha$  (G) messenger RNA (mRNA) levels in liver extracts were measured by quantitative reverse-transcription polymerase chain reaction (PCR). Representative images of immunohistochemistry for serine 536 phosphorylation of nuclear factor kappa B (NF- $\kappa$ B) (H) and tyrosine 705 phosphorylation of signal transducer and activator of transcription 3 (STAT3) (I) in liver tissues from mice. Brown dots indicate positive staining in nuclei. Values are expressed as mean  $\pm$  SEM. Statistics were performed using Student's *t* test. \**p* < 0.05, \*\**p* < 0.01.

Alb-Cre mice (Figure 3H,I). The data indicated that PLC $\gamma$ 1 contributes to liver inflammation and damage.

### NF- $\kappa$ B/IL-6/STAT3 axis and HCC cell proliferation are promoted by PLC $\gamma$ 1

Next, we explored the mechanisms underlying the oncogenic role of PLC $\gamma$ 1 in HCC. Based on the results

of our *in vivo* experiments, we expected that PLC $\gamma$ 1 would regulate the NF- $\kappa$ B/IL-6/STAT3 axis in HCC. Crosstalk between NF- $\kappa$ B and STAT3 has an oncogenic role in some cancer types.<sup>[17,18]</sup> To investigate the potential oncogenic function and mechanism of PLC $\gamma$ 1 in human HCC, we constructed Hep3B and Huh7 cell lines stably overexpressing PLC $\gamma$ 1 (Figure 3A). To analyze the effects of PLC $\gamma$ 1 deficiency, we used specific siRNA against the PLC $\gamma$ 1

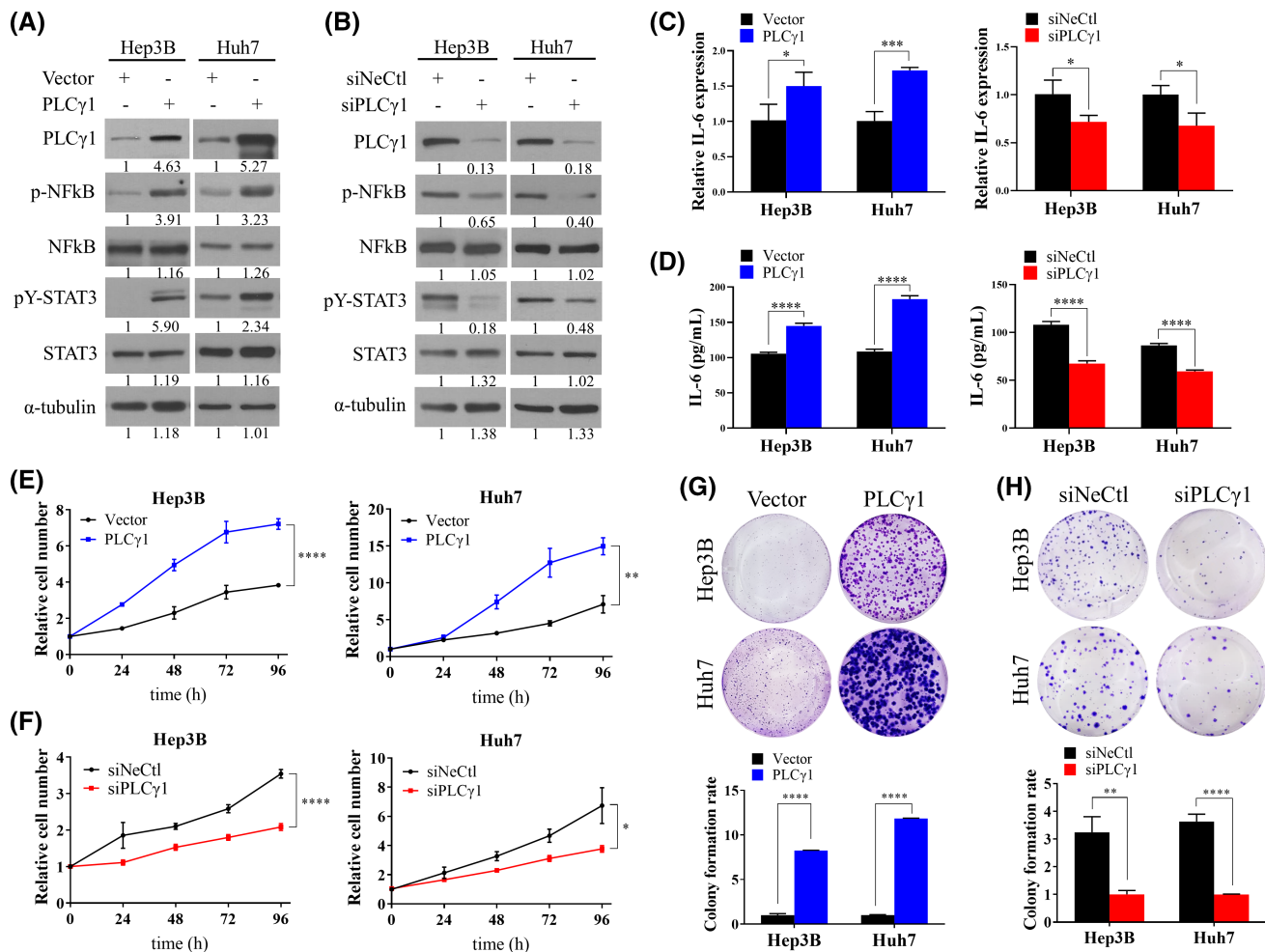


**FIGURE 3** NF- $\kappa$ B/IL-6/STAT3 axis and HCC cell proliferation are promoted by PLC $\gamma$ 1. (A) Hep3B and Huh7 cells were transfected with either the empty vector or PLC $\gamma$ 1 expression vector and selected with G418. Overexpression of PLC $\gamma$ 1 and downstream signals were confirmed by western blot analysis. (B) Hep3B and Huh7 cells were either transfected with the negative control (siNeCtl) or PLC $\gamma$ 1 targeting (siPLC $\gamma$ 1) small interfering RNAs. Down-regulation of PLC $\gamma$ 1 and related target protein expressions were confirmed by western blot analysis. (C) IL-6 mRNA levels in cell lysates were quantified by quantitative reverse-transcription polymerase chain reaction (PCR). (D) IL-6 cytokine levels in supernatant culture medium were measured by ELISA. (E, F) Cell proliferation rates of HCC cells with different PLC $\gamma$ 1 levels. (G, H) Representative images of colony formation assays and quantitative analysis of colony-forming ability based on crystal violet staining. All values are expressed as mean  $\pm$  SD ( $n = 3$ ). Statistics were performed using Student's  $t$  test. \* $p < 0.05$ , \*\* $p < 0.01$ , \*\*\* $p < 0.001$ , and \*\*\*\* $p < 0.0001$ .

gene transcript (Figure 3B). Immunoblotting analysis showed that PLC $\gamma$ 1 activates phosphorylation of both the NF- $\kappa$ B and STAT3 proteins (Figure 3A, B; Figure S5A–F). In addition, both intracellular IL-6 mRNA expression (Figure 3C) and IL-6 cytokine levels released into the supernatant medium were positively regulated by PLC $\gamma$ 1 (Figure 3D). Next, we examined the phenotypes expressed by PLC $\gamma$ 1 in human HCC cell lines. Growth curves demonstrated that up-regulation of PLC $\gamma$ 1 significantly promoted Hep3B and Huh7 cell growth (Figure 3E), but down-regulation of PLC $\gamma$ 1 decreased HCC cell growth compared with the negative control (Figure 3F). In the colony formation assay, PLC $\gamma$ 1 increased the colony-forming ability of HCC cells (Figure 3G), whereas silencing of PLC $\gamma$ 1 led to a decrease in the clonogenic

survival of the cells (Figure 3H). These results demonstrated that PLC $\gamma$ 1 affects tumorigenesis by promoting HCC cell proliferation.

### PLC $\gamma$ 1 plays a critical role in accelerating cell cycle progression and inhibiting apoptosis

Flow cytometric analyses were performed to determine whether PLC $\gamma$ 1 affects the cell cycle or cell death. Fluorescence-activated cell sorting (FACS) analysis showed that PLC $\gamma$ 1 contributes to the cell cycle phase. HCC cells overexpressing PLC $\gamma$ 1 had an increased population of S phase cells and an accompanying decrease in G1 phase cells (Figure 4A). In

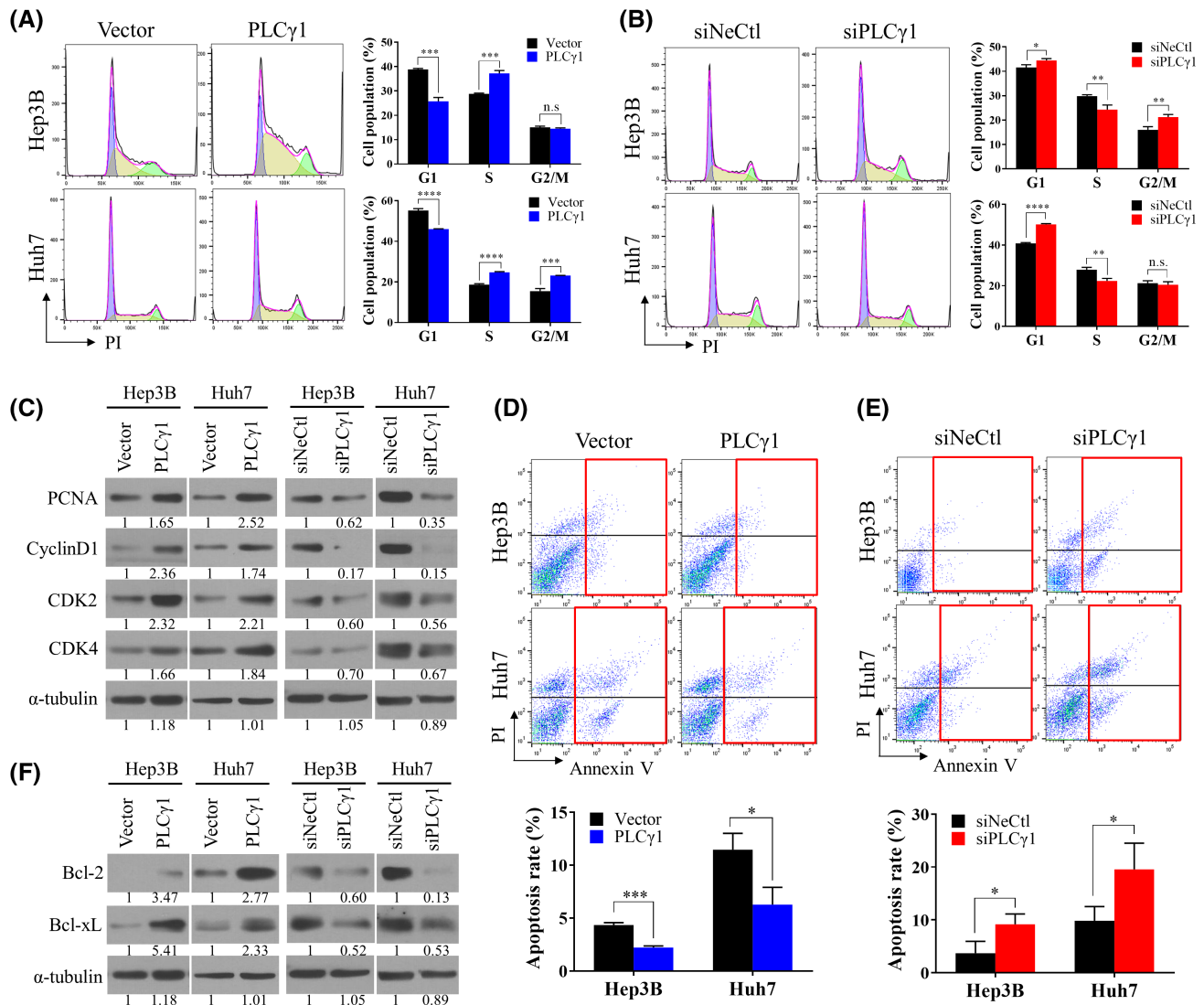


**FIGURE 4** PLC $\gamma$ 1 plays a critical role in accelerating cell cycle progression and inhibiting apoptosis. (A,B) Cell cycle analysis in HCC cells and quantitative measurement of cell populations at each cell cycle phase. Cells were stained with propidium iodide (PI) and analyzed by flow cytometry. (C) Cell cycle-related protein-expression levels detected by western blot analysis following PLC $\gamma$ 1 levels. (D,E) Apoptosis assay and statistical analysis of apoptosis rates in HCC cell lines with different PLC $\gamma$ 1 levels. Cells were stained with annexin V-fluorescein isothiocyanate (V-FITC) and propidium iodide (PI) and analyzed by flow cytometry. (F) Expression levels of anti-apoptotic proteins detected by western blot analysis following PLC $\gamma$ 1 levels. All values are expressed as mean  $\pm$  SD (n = 3). Statistics were performed using Student's *t* test. \* $p$  < 0.05, \*\* $p$  < 0.01, \*\*\* $p$  < 0.001 and \*\*\*\* $p$  < 0.0001. n.s., not significant.

contrast, PLC $\gamma$ 1 knockdown in HCC cells induced G1 arrest (Figure 4B). Consistent with these observations, PLC $\gamma$ 1 regulated the expression of PCNA, CyclinD1, CDK2, and CDK4, which are cell cycle-related proteins required for the G1 to S-phase transition (Figure 4C; Figure S6A–H). These results indicated that PLC $\gamma$ 1 accelerates cell cycle progression from G1 to the S phase. FACS analysis also showed that PLC $\gamma$ 1 regulates apoptosis. The percentage of apoptotic cells decreased when PLC $\gamma$ 1 was up-regulated (Figure 4D), whereas down-regulation of PLC $\gamma$ 1 induced apoptosis (Figure 4E). In addition, PLC $\gamma$ 1 induced expression of the anti-apoptotic proteins Bcl-2 and Bcl-xL (Figure 4F; Figure S7A–D). Briefly, these results suggest that

PLC $\gamma$ 1 promotes tumorigenesis by facilitating cell cycle progression and inhibiting apoptosis in HCC.

### Metastatic potential is enhanced by PLC $\gamma$ 1-mediated epithelial–mesenchymal transition

PLC $\gamma$ 1 plays a critical role in promoting metastasis in several cancers as well as regulating tumor growth.<sup>[11–13]</sup> In our *in vivo* experiments, lung lesion was observed only in DEN-treated male WT mice (Figure S8A–C). In addition, the function of PLC $\gamma$ 1 in HCC for metastasis, a representative phenotype of malignant tumors,



has not been well elucidated. Therefore, we then explored the metastatic activity of PLC $\gamma$ 1 in hepatocytes. To investigate whether PLC $\gamma$ 1 affects tumor metastasis in HCC, we analyzed differences in cell migration and invasion based on the PLC $\gamma$ 1 protein levels. We performed a Transwell assay to assess cell migration, and Matrigel-coated Transwell chambers were used to assess cell invasion. A Transwell assay showed that up-regulation of PLC $\gamma$ 1 markedly increased the migration and invasion of Hep3B and Huh7 cells (Figure 5A).

Conversely, PLC $\gamma$ 1 silencing effectively inhibited cell migration and invasion compared with the negative control (Figure 5B). Consistent with the Transwell assay results, a wound-healing assay showed that cell motility was increased in HCC cells overexpressing PLC $\gamma$ 1 (Figure 5C) but decreased by PLC $\gamma$ 1 knock-down (Figure 5D). In line with these results, PLC $\gamma$ 1 regulated the expression of Snail and matrix metalloproteinase 2 (MMP2), which are closely linked to metastasis (Figure 5E; Figure S9A–D). Furthermore, we

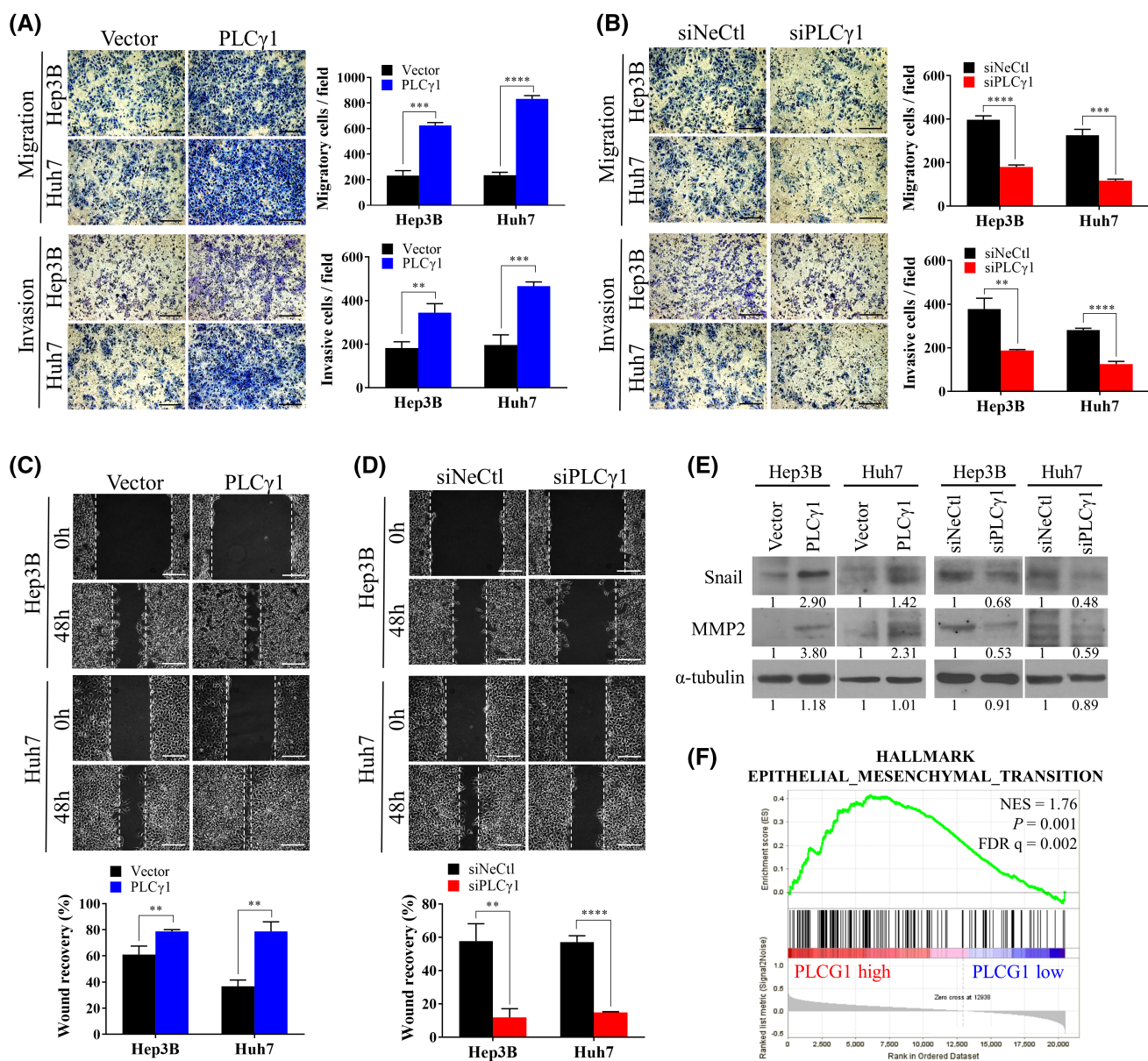


**FIGURE 5** Metastatic potential is enhanced by PLC $\gamma$ 1-mediated epithelial–mesenchymal transition (EMT). (A,B) Representative images and statistical plots of Transwell migration assays and Transwell Matrigel-coated invasion assays. Migratory or invasive cells were stained with crystal violet. Scale bar: 200  $\mu$ m. (C,D) Representative images and statistical plots of wound-healing assays in HCC cells. Scale bar: 200  $\mu$ m. (E) Protein expression levels of Snail and matrix metalloproteinase 2 (MMP2) following PLC $\gamma$ 1 levels detected by western blot analysis. All values are expressed as mean  $\pm$  SD (n = 3). Statistics were performed using Student's *t* test. \*\**p* < 0.01, \*\*\**p* < 0.001 and \*\*\*\**p* < 0.0001. (F) Gene Set Enrichment Analysis (GSEA) enrichment plot of the EMT gene set positively correlated with the PLCG1-high group. Data sets derived from patients with HCC were imported from The Cancer Genome Atlas (TCGA) and divided into two groups according to the levels of PLCG1 mRNA expression. FDR, false discovery rate; NES, normalized enrichment score.

performed a Gene Set Enrichment Analysis (GSEA) on the Cancer Genome Atlas (TCGA) data sets to confirm the association between PLC $\gamma$ 1 and metastasis in HCC. Patients with HCC were sorted into PLCG1-high and PLCG1-low groups based on the median expression levels (Figure S10A). The PLCG1-high group showed positive correlations with the epithelial–mesenchymal transition (EMT)–related gene sets (Figure 5F). The same results were confirmed when analyzing the Genomic Spatial Event (GSE) database (Figure S10B,C). These results demonstrated the crucial role played by PLC $\gamma$ 1 in promoting cell metastasis in HCC.

## PLC $\gamma$ 1 is an essential target molecule as a clinical biomarker for HCC

To ascertain the clinical relevance of PLC $\gamma$ 1 in HCC, PLC $\gamma$ 1 expression in human liver samples of patients with HCC was analyzed by immunohistochemistry. Immunostaining analysis demonstrated that the PLC $\gamma$ 1 and active STAT3 levels were significantly elevated in HCC tissues compared with adjacent non-cancerous tissues (Figure 6A). To fully explore these results, we compared PLC $\gamma$ 1 expression between normal and HCC samples using the GSE databases. All of the data sets showed that PLC $\gamma$ 1 mRNA levels

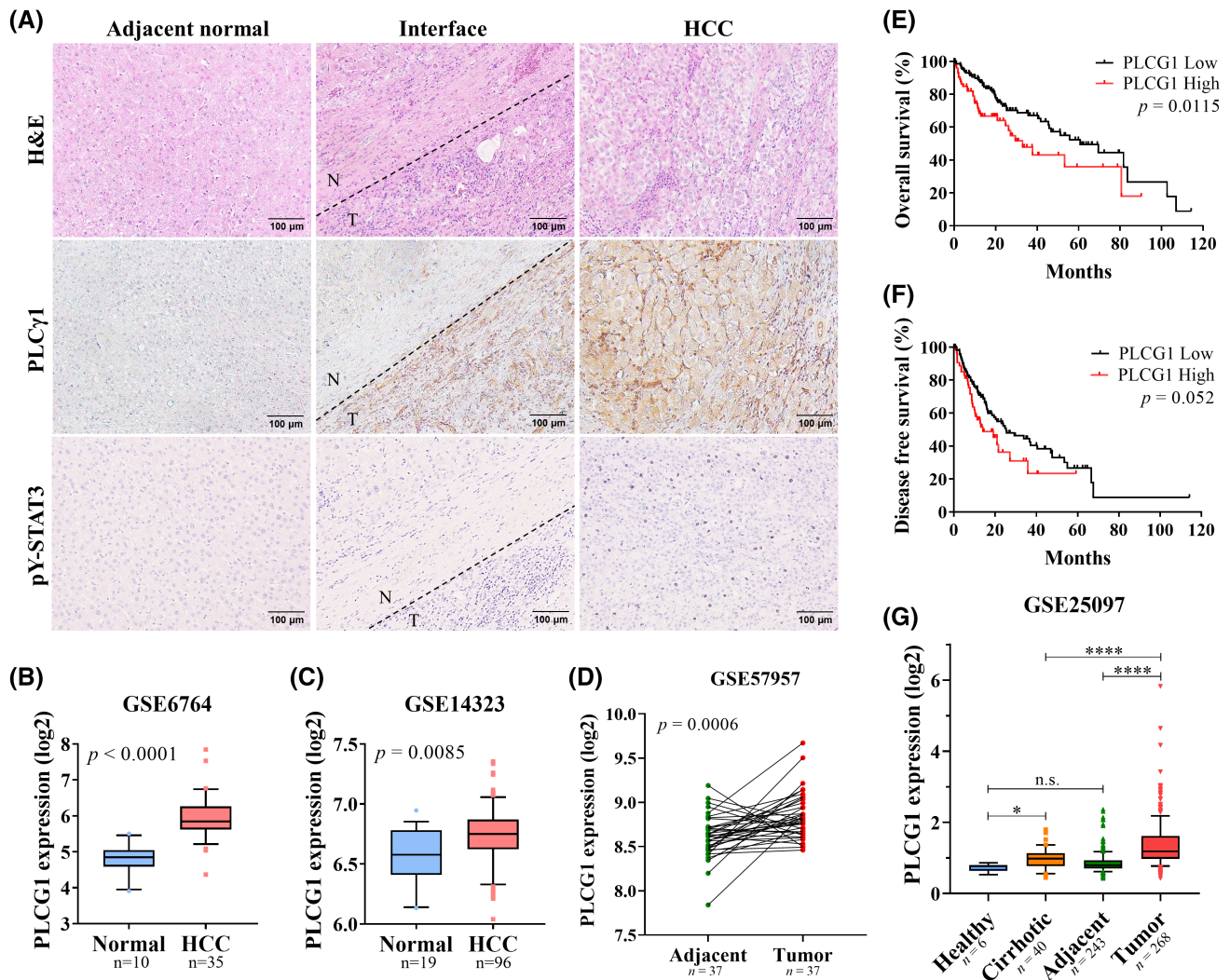


**FIGURE 6** PLC $\gamma$ 1 expression is elevated in human HCC and correlates with poor prognosis in patients with HCC. (A) Representative images of hematoxylin and eosin (H&E) staining and immunohistochemistry for PLC $\gamma$ 1 and pY-STAT3 in human liver tissues that contained HCC and adjacent normal tissues. Dashed lines present the border between tumor region and adjacent nontumor. Brown color indicates positive staining. PLC $\gamma$ 1 mRNA levels in normal and HCC liver tissue samples from the GSE6764 (B) and GSE14313 (C) data sets. Horizontal lines represent the median values. Boxes and whiskers represent 25–75 and 10–90 percentiles, respectively. The  $p$  value was calculated by Mann-Whitney test. (D) PLC $\gamma$ 1 mRNA expression levels in 37 pairs of adjacent nontumor tissues versus tumors in patients with HCC from the GSE57957 data set. The  $p$  value was calculated by paired two-tailed  $t$  test. (E) Kaplan-Meier analysis of overall survival (E) and disease-free survival (F) of patients with HCC were performed in PLCG1-high and PLCG1-low groups. The  $p$  value was calculated by log-rank test. (G) PLC $\gamma$ 1 mRNA expression levels of healthy liver, cirrhosis, HCC, and adjacent nontumor tissues from the GSE25097 data set. The  $p$  value was calculated by Mann-Whitney test.

were significantly elevated in the HCC samples compared with the healthy subjects (Figure 6B,C). In addition, PLC $\gamma$ 1 expression was significantly increased in tumors compared with adjacent normal tissue pairs in patients with HCC (Figure 6D). Next, to determine whether PLC $\gamma$ 1 levels affected the prognosis of patients with HCC, survival analysis was performed using the TCGA database. Patients with HCC were classified into PLCG1-high and PLCG1-low groups based on the mean PLCG1 expression levels (Figure S10A). Both OS and DFS were lower in the PLCG1-high group compared with the PLCG1-low group (Figure 6E,F). Kaplan–Meier and log-rank analyses indicated that patients with HCC with high PLC $\gamma$ 1 expression had a reduced OS rate and higher recurrence rate relative to patients with low PLC $\gamma$ 1 expression. Moreover, the expression of PLC $\gamma$ 1 showed a tendency to progressively increase in pathological stage (Figure 6G). Overall, these results imply that overexpression of PLC $\gamma$ 1 plays a key role in the development and progression of human HCC.

## DISCUSSION

PLC $\gamma$ 1 is oncogenic in some cancer types,<sup>[19–21]</sup> liver cancer being a major cancer type; however, the understanding of the function of PLC $\gamma$ 1 in liver cancer is very poor. Based on results from other studies, we expected PLC $\gamma$ 1 to function as an oncogene in liver cancer, such that clarification of its role is essential for the diagnosis and treatment of liver cancer. We aimed to understand the pathological role of PLC $\gamma$ 1 in liver cancer, and to determine the phenotype of liver cancer caused by PLC $\gamma$ 1.

In this study, we generated a transgenic mouse model to demonstrate the function of PLC $\gamma$ 1 in HCC. In Alb-Cre mice, PLC $\gamma$ 1 was knocked out specifically in hepatocytes, as PLC $\gamma$ 1 is essential for embryonic development, and examined its role in the liver.<sup>[15]</sup> Next, we used DEN to induce HCC in rodents.<sup>[22,23]</sup> DEN treatment mimics spontaneous HCC of human by causing DNA damage, the accumulation of which can stimulate the inflammatory response and hyperproliferation that support tumor development.<sup>[24,25]</sup> Our results showed that deletion of PLC $\gamma$ 1 led to dramatically attenuated hepatocarcinogenesis, HCC progression, and proliferative responses in tumors.

Inflammation is a key factor in various types of cancer; in particular, it is the main inducer of liver cancer.<sup>[26,27]</sup> Recent studies reinforced the notion that tumors are promoted by inflammatory signals in the surrounding tumor microenvironment.<sup>[28,29]</sup> In this study, we demonstrated that ablation of PLC $\gamma$ 1 markedly attenuated the histopathological inflammatory response in liver tumors of mice, and led to a decrease in the production of the inflammatory cytokines IL-6

and TNF- $\alpha$ . These typical liver inflammatory cytokines stimulate inflammation and autoimmune responses in many diseases.<sup>[30]</sup> Previous studies reported higher IL-6 levels in cases of HCC,<sup>[31]</sup> and the up-regulation of IL-6 increased inflammation through infiltration of immune cells.<sup>[32]</sup> Of note, ablation of PLC $\gamma$ 1 also suppressed both NF- $\kappa$ B and STAT3 activation in hepatocytes. NF- $\kappa$ B serves as a pivotal mediator of inflammatory responses by inducing the expression of various pro-inflammatory genes.<sup>[33]</sup> STAT3, which is frequently activated in malignant cells, regulates many genes important for cancer inflammation in the tumor microenvironment.<sup>[34]</sup> Furthermore, higher serum ALT and AST levels indicated more severe liver injury in a group of WT mice.<sup>[35]</sup>

The data presented were collected from male mice due to the estrogen-mediated inhibitory mechanism that occurs in females.<sup>[36]</sup> Tumors did not develop in females, but PLC $\gamma$ 1 deficiency relieved the formation of dysplastic hepatocytes and hepatic inflammatory responses. As an extension of the *in vitro* experiment, we note that metastasis occurred only in WT mice and not in PLC $\gamma$ 1<sup>fl/fl</sup>; Alb-Cre mice, although this difference was not statistically significant.

To investigate the function of PLC $\gamma$ 1 fully *in vitro*, we used stable cells and silencing systems in human HCC cell lines. Based on *in vivo* experimental results, we explored proliferation, cell cycle, and apoptosis in HCC cell lines. Our results showed that PLC $\gamma$ 1 promotes HCC cell growth and cell cycle progression, but prevents apoptosis. In metastasis, PLC $\gamma$ 1 mediated the migration and invasion of HCC cells. GSEA analysis of the gene set associated with PLC $\gamma$ 1 showed that PLC $\gamma$ 1 positively correlated with genes associated with the EMT. Our data also confirmed that PLC $\gamma$ 1 regulates the expression of the signaling proteins associated with these phenotypes.

STAT3 is a key molecule transducing signals from a variety of factors, including IL-6.<sup>[37]</sup> It is reported that IL-6 acts as an autocrine growth factor in human prostate cancer.<sup>[38]</sup> Several studies have demonstrated that abnormal IL-6/STAT3 signaling promotes HCC progression.<sup>[39]</sup> In our previous study, it was reported that IL-6/STAT3 signaling induces cancer stemness through up-regulation of CD133 expression during liver carcinogenesis.<sup>[40]</sup> We confirmed in this study that PLC $\gamma$ 1-mediated STAT3 activation is involved in metastatic potential of HCC cells. Furthermore, IL-6 is an NF- $\kappa$ B-dependent tumor growth factor,<sup>[41]</sup> and its production is positively regulated by NF- $\kappa$ B activation.<sup>[42]</sup> In addition, NF- $\kappa$ B is activated by PKC downstream of PLC $\gamma$ 1.<sup>[43,44]</sup> Based on these research backgrounds, we hypothesized that PLC $\gamma$ 1 could regulate the activation of STAT3 via the NF- $\kappa$ B/IL-6/STAT3 axis. A recent study reported crosstalk between STAT3 and PLC $\gamma$ 1 in colorectal cancer.<sup>[45]</sup> However, studies on whether PLC $\gamma$ 1 can regulate the activity of STAT3 are lacking, and the relationship

between PLC $\gamma$ 1 and STAT3 associated with liver cancer is still unknown. In the present study, serum IL-6 and IL-6 mRNA levels in liver extracts were decreased in PLC $\gamma$ 1<sup>ff</sup>; Alb-Cre mice, in which NF- $\kappa$ B and STAT3 activation were also inhibited in hepatocytes. In our *in vitro* study, PLC $\gamma$ 1 induced phosphorylation of NF- $\kappa$ B and STAT3 in human HCC cell lines. In addition, both intracellular IL-6 expression and extracellularly secreted IL-6 cytokine levels were positively regulated by PLC $\gamma$ 1. Moreover, proteins that underwent phenotype testing, such as cyclin D1, Bcl-2, Bcl-xL, Snail and MMP2, were STAT3 downstream target genes. Thus, we suggest that PLC $\gamma$ 1 regulates the activation of STAT3 as a possible mechanism promoting HCC progression. Further studies are needed to determine the detailed mechanisms of PLC $\gamma$ 1 signaling in HCC and to understand the regulation of the pathway.

Additionally, a clinical approach using human liver tissue verified that PLC $\gamma$ 1 and activated STAT3 were highly expressed in liver cancer cells compared with adjacent normal liver cells. We confirmed the clinical relevance of this through bioinformatics analysis using the TCGA database. The expression of PLC $\gamma$ 1 was higher in patients with HCC compared to the normal group, indicating that PLC $\gamma$ 1 is associated with the development of HCC. The study of patients with HCC showed that both OS and DFS were poor in the PLC $\gamma$ 1-high expression group, suggesting that PLC $\gamma$ 1 is also associated with the progression and relapse of HCC. This finding supports the results observed in the current study.

## CONCLUSIONS

In this study, we suggested that PLC $\gamma$ 1 is a key molecule in hepatocellular carcinogenesis and progression. Loss of PLC $\gamma$ 1 efficiently attenuated the tumor growth and inflammatory responses in the tumor microenvironment. Moreover, PLC $\gamma$ 1 induced representative oncogenic phenotypes and expression of corresponding factors in human HCC cells. The PLC $\gamma$ 1/STAT3 axis is a potential therapeutic target pathway with oncogenic function in HCC. Thus, our findings could inform strategies for the treatment and prognostic diagnosis of HCC.

## AUTHOR CONTRIBUTIONS

*Study design and experiments:* Eun-Bi Seo. *Discussion of the results:* Sun-Ho Kwon and Yong-Jin Kwon. *Data collection:* Seul-Ki Kim, Song-Hee Lee, and Ae Jin Jeong. *Data analysis:* Hyun Mu Shin, Yong-Nyun Kim, and Stephanie Ma. *Generation of mice:* Hyun-Jun Jang and Pann-Ghill Suh. *Clinical resources:* Haeryoung Kim. *Study concept:* Sang-Kyu Ye. *Data interpretation:* Yun-Han Lee. *Manuscript draft:* Eun-Bi Seo. *Manuscript review:* Sang-Kyu Ye. All authors had final approval of the submitted and published versions.

## ACKNOWLEDGMENT

The authors thank Dr. Byung-Hak Kim for the discussion of animal studies, and Dr. Iljin Kim for the advice on bioinformatics analysis.

## FUNDING INFORMATION

Supported by the National Research Foundation of Korea grant funded by the Korean Government (NRF-2018R1A5A2025964 and NRF-2022R1A2C1011914); Seoul National University Hospital Research Fund (0420200230); R&D Program for Forest Science Technology (2020195A00-2122-BA01) provided by the Korea Forest Service (Korea Forestry Promotion Institute); and Cooperative Research Program for Agriculture Science and Technology Development (PJ01602001 and PJ01589402) provided by Rural Development Administration, Republic of Korea.

## CONFLICT OF INTEREST

Nothing to report.

## ORCID

Stephanie Ma  <https://orcid.org/0000-0002-2029-7943>

## REFERENCES

- Villanueva A. Hepatocellular carcinoma. *N Engl J Med.* 2019;380:1450–62.
- Siegel RL, Miller KD, Jemal A. Cancer statistics, 2019. *CA Cancer J Clin.* 2019;69:7–34.
- Yang JD, Hainaut P, Gores GJ, Amadou A, Plymoth A, Roberts LR. A global view of hepatocellular carcinoma: trends, risk, prevention and management. *Nat Rev Gastroenterol Hepatol.* 2019;16:589–604. <https://doi.org/10.1038/s41575-019-0186-y>
- Vogel A, Martinelli E, Cervantes A, Chau I, Daniele B, Llovet JM, et al. Updated treatment recommendations for hepatocellular carcinoma (HCC) from the ESMO Clinical Practice Guidelines. *Ann Oncol.* 2021;32:801–5.
- Gilsanz GV. Hepato-cellular carcinoma. *Ann Gastroenterol Hepatol (Paris).* 1989;25:267–75.
- Rebecchi MJ, Pentylala SN. Structure, function, and control of phosphoinositide-specific phospholipase C. *Physiol Rev.* 2000;80:1291–335.
- Berridge MJ. Inositol trisphosphate and calcium signalling. *Nature.* 1993;361:315–25.
- Nakamura Y, Fukami K. Regulation and physiological functions of mammalian phospholipase C. *J Biochem.* 2017;161:315–21.
- Arteaga CL, Johnson MD, Todderud G, Coffey RJ, Carpenter G, Page DL. Elevated content of the tyrosine kinase substrate phospholipase C- $\gamma$ 1 in primary human breast carcinomas. *Proc Natl Acad Sci U S A.* 1991;88:10435–9.
- Nomoto M, Tomita N, Miyake M, Xhu D-B, Logerfo PR, Weinstein IB. Expression of phospholipases  $\gamma$ 1,  $\beta$ 1, and  $\delta$ 1 in primary human colon carcinomas and colon carcinoma cell lines. *Mol Carcinog.* 1995;12:146–52.
- Zhuang L, Zhang B, Zeng G, Dai L, Qian H, Hu T, et al. Metastasis of human gastric adenocarcinoma partly depends on phosphoinositide-specific phospholipase  $\gamma$ 1 expression. *Folia Histochem Cytobiol.* 2014;52:178–86.
- Sala G, Dituri F, Raimondi C, Previdi S, Maffucci T, Mazzeletti M, et al. Phospholipase C $\gamma$ 1 is required for metastasis development and progression. *Cancer Res.* 2008;68:10187–96.

13. Shepard CR, Kassis J, Whaley DL, Kim HG, Wells A. PLC $\gamma$  contributes to metastasis of in situ-occurring mammary and prostate tumors. *Oncogene*. 2007;26:3020–6.
14. Tang W, Zhou Y, Sun D, Dong L, Xia J, Yang B. Oncogenic role of phospholipase C- $\gamma$ 1 in progression of hepatocellular carcinoma. *Hepatol Res*. 2019;49:559–69.
15. Ji QS, Winnier GE, Niswender KD, Horstman D, Wisdom R, Magnuson MA, et al. Essential role of the tyrosine kinase substrate phospholipase C- $\gamma$ 1 in mammalian growth and development. *Proc Natl Acad Sci U S A*. 1997;94:2999–3003.
16. Yang YR, Jung JH, Kim SJ, Hamada K, Suzuki A, Kim HJ, et al. Forebrain-specific ablation of phospholipase C $\gamma$ 1 causes manic-like behavior. *Mol Psychiatry*. 2017;22:1473–82.
17. McFarland BC, Hong SW, Rajbhandari R, Twitty GB, Gray GK, Yu H, et al. NF- $\kappa$ B-induced IL-6 ensures STAT3 activation and tumor aggressiveness in glioblastoma. *PLoS One*. 2013;8:e78728.
18. Squarize CH, Castilho RM, Sriuranpong V, Pinto DS, Gutkind JS. Molecular cross-talk between the NF $\kappa$ B and STAT3 signaling pathways in head and neck squamous cell carcinoma. *Neoplasia*. 2006;8:733–46.
19. Nozawa H, Howell G, Suzuki S, Zhang Q, Qi Y, Klein-Seetharaman J, et al. Combined inhibition of PLC $\gamma$ -1 and c-Src abrogates epidermal growth factor receptor-mediated head and neck squamous cell carcinoma invasion. *Clin Cancer Res*. 2008;14:4336–44.
20. Vaqué JP, Gómez-López G, Monsálvez V, Varela I, Martínez N, Pérez C, et al. PLCG1 mutations in cutaneous T-cell lymphomas. *Blood*. 2014;123:2034–43.
21. Behjati S, Tarpey PS, Sheldon H, Martincorena I, Van Loo P, Gundem G, et al. Recurrent PTPRB and PLCG1 mutations in angiosarcoma. *Nat Genet*. 2014;46:376–9.
22. Chen L, Park SM, Tumanov AV, Hau A, Sawada K, Feig C, et al. CD95 promotes tumour growth. *Nature*. 2010;465:492–6.
23. Bard-Chapeau EA, Li S, Ding J, Zhang SS, Zhu HH, Princen F, et al. Ptpn11/Shp2 acts as a tumor suppressor in hepatocellular carcinogenesis. *Cancer Cell*. 2011;19:629–39.
24. Vesselinovich SD, Koka M, Mihailovich N, Rao KVN. Carcinogenicity of diethylnitrosamine in newborn, infant, and adult mice. *J Cancer Res Clin Oncol*. 1984;108:60–5.
25. Verna L, Whysner J, Williams GM. N-Nitrosodiethylamine mechanistic data and risk assessment: bioactivation, DNA-adduct formation, mutagenicity, and tumor initiation. *Pharmacol Ther*. 1996;71:57–81.
26. Mantovani A, Allavena P, Sica A, Balkwill F. Cancer-related inflammation. *Nature*. 2008;454:436–44.
27. Cheng J, Zhong Y, Chen S, Sun Y, Huang L, Kang Y, et al. Gab2 mediates hepatocellular carcinogenesis by integrating multiple signaling pathways. *FASEB J*. 2017;31:5530–42.
28. Coussens LM, Werb Z. Inflammation and cancer. *Nature*. 2002;420:860–7.
29. Yu H, Kortylewski M, Pardoll D. Crosstalk between cancer and immune cells: role of STAT3 in the tumour microenvironment. *Nat Rev Immunol*. 2007;7:41–51.
30. Grivennikov SI, Greten FR, Karin M. Immunity, Inflammation, and Cancer. *Cell*. 2010;140:883–99.
31. Grivennikov SI, Karin M. Dangerous liaisons: STAT3 and NF- $\kappa$ B collaboration and crosstalk in cancer. *Cytokine Growth Factor Rev*. 2010;21:11–9.
32. Grivennikov S, Karin M. Autocrine IL-6 signaling: a key event in tumorigenesis? *Cancer Cell*. 2008;13:7–9.
33. Liu T, Zhang L, Joo D, Sun SC. NF- $\kappa$ B signaling in inflammation. *Signal Transduct Target Ther*. 2017;2:17023.
34. Yu H, Pardoll D, Jove R. STATs in cancer inflammation and immunity: a leading role for STAT3. *Nat Rev Cancer*. 2009;9:798–809.
35. Shalini S, Nikolic A, Wilson CH, Puccini J, Sladojevic N, Finnie J, et al. Caspase-2 deficiency accelerates chemically induced liver cancer in mice. *Cell Death Differ*. 2016;23:1727–36.
36. De MN, Manno M, Villa E. Sex hormones and liver cancer. *Mol Cell Endocrinol*. 2002;193:59–63.
37. Bromberg J, Wang TC. Inflammation and Cancer: IL-6 and STAT3 complete the link. *Cancer Cell*. 2009;15:79–80.
38. Giri D, Ozen M, Ittmann M. Interleukin-6 is an autocrine growth factor in human prostate cancer. *Am J Pathol*. 2001;159:2159–65.
39. He G, Karin M. NF- $\kappa$ B and STAT3—key players in liver inflammation and cancer. *Cell Res*. 2011;21:159–68.
40. Won C, Kim BH, Yi EH, Choi KJ, Kim EK, Jeong JM, et al. Signal transducer and activator of transcription 3-mediated CD133 up-regulation contributes to promotion of hepatocellular carcinoma. *Hepatology*. 2015;62:1160–73.
41. Grivennikov S, Karin E, Terzić J, Mucida D, Yu GY, Vallabhapurapu S, et al. IL-6 and Stat3 are required for survival of intestinal epithelial cells and development of colitis-associated cancer. *Cancer Cell*. 2009;15:103–13.
42. Rego D, Kumar A, Nilchi L, Wright K, Huang S, Kozlowski M. IL-6 production is positively regulated by two distinct Src homology domain 2-containing tyrosine phosphatase-1 (SHP-1)-dependent CCAAT/enhancer-binding protein  $\beta$  and NF- $\kappa$ B pathways and an SHP-1-independent NF- $\kappa$ B pathway in lipopolysaccharide-stimulated bone marrow-derived macrophages. *J Immunol*. 2011;186:5443–56.
43. Shostak K, Chariot A. EGFR and NF- $\kappa$ B: partners in cancer. *Trends Mol Med*. 2015;21:385–93.
44. Rakonczay Z, Hegyi P, Takács T, McCarroll J, Saluja AK. The role of NF- $\kappa$ B activation in the pathogenesis of acute pancreatitis. *Gut*. 2008;57:259–67.
45. Zhang P, Zhao Y, Zhu X, Sedwick D, Zhang X, Wang Z. Crosstalk between phospho-STAT3 and PLC $\gamma$ 1 plays a critical role in colorectal tumorigenesis. *Mol Cancer Res*. 2011;9:1418–28.

## SUPPORTING INFORMATION

Additional supporting information can be found online in the Supporting Information section at the end of this article.

**How to cite this article:** Seo E-B, Jang H-J, Kwon S-H, Kwon Y-J, Kim S-K, Lee S-H, et al. Loss of phospholipase C $\gamma$ 1 suppresses hepatocellular carcinogenesis through blockade of STAT3-mediated cancer development. *Hepatol Commun*. 2022;6:3234–3246. <https://doi.org/10.1002/hep4.2077>